2010

A Parametric Analysis for the Impact of Facade Design Options on the Daylighting Performance of Office Spaces

Hui Shen
Purdue University

Athanasios Tzempelikos
Purdue University

A Parametric Analysis for the Impact of Facade Design Options on the Daylighting Performance of Office Spaces

Hui SHEN[1]*, Athanasios TZEMPELIKOS[1]

[1]Purdue University, School of Civil Engineering, West Lafayette, Indiana, USA
Tel.: 765-496-7586, Fax: 765-494-0395, E-mail: shen34@purdue.edu

* Corresponding Author

ABSTRACT

This paper presents a calculation model that combines the radiosity method with one-bounce ray-tracing for prediction of hourly indoor illuminances and annual advanced daylighting metrics. Using dynamic (variable) view factors for computing inter-reflections between variable surfaces, these metrics are presented as a function of façade parameters (window size, properties, orientation and geometry) in order to help the designers make better decisions related to optimal daylighting performance. High accuracy without compromising for computational speed was achieved using specific simplifications. Results are presented for different climatic locations in the US to include the impact of weather conditions. In all locations, daylight "saturation" is observed for window-to-wall ratios higher than 40%. Investigation of useful daylight illuminances and percentage of sunlit area throughout the year are also presented for a deeper analysis. This model will be further developed to include the impact of shading and will be combined with a dynamic thermal model for overall evaluation of façade design options.

1. INTRODUCTION

Windows are the most critical components of commercial building facades. Their shape, size and optical properties determine indoor daylighting conditions and visual comfort (Reinhart, 2002; Tzempelikos and Athienitis, 2007). Optimized glass façade design may improve exploitation of daylight and result in significant savings in electricity consumption for lighting (Tzempelikos and Athienitis, 2002, 2007). On the other hand, computational models that consider comprehensive building simulation are needed for prediction of illuminance on the interior surfaces of a building as well as on the work plane level (Rosa *et al.*, 2009). Although various calculation models are available (Carrol, 1999; Mardajevic, 2001; Ward and Shakespeare, 2003), they usually have some limitations in room geometry inputs, sky luminance inputs or evaluation metrics (Rosa *et al.*, 2009; Nabil and Mardaljevic, 2006). Moreover, it is complicated to modify existing codes to adapt specific necessities or present results using different measures. As to the latter, advanced daylighting metrics may be properly used in daylighting performance evaluation (Nabil and Mardaljevic, 2006; Reinhart *et al*., 2006).

This paper presents a flexible daylighting simulation model for calculation of hourly illuminance values on any interior surface. The model uses a combined one-bounce ray-tracing and radiosity method for computation of illuminance values. Daylighting metrics such as daylight autonomy and useful daylight illuminances are computed as a function of façade parameters (window size, properties, orientation and geometry) for different climatic locations in the US. This model will be further developed to include the impact of shading and will be combined with a dynamic thermal model for overall evaluation of façade design options.

2. DAYLIGHTING CALCULATION MODEL

2.1 Incident and transmitted illuminance

Direct and diffuse illuminance from the sky and the ground are calculated separately using the Perez luminous efficacy model (Perez *et al*., 1990). The input data of Perez model including hourly beam normal irradiance, beam and diffuse horizontal irradiance and dew-point temperature were obtained from TMY3 weather data. The output of the model is hourly direct and diffuse illuminance on the façade. After calculation of direct and diffuse incident

illuminance on the windows, the transmitted daylight is computed by multiplying the hourly values with the respective varying glass visible transmittance. Beam transmittance is input as a function of the solar incidence angle (Figure 3), whereas diffuse transmittance is set equal to the beam transmittance for incidence angle equal to 60^0.

2.2 Interior surface luminous exitance and illuminance on the work plane

The model calculates directly transmitted daylight and diffuse incoming light at each time step (=1 hour). For direct transmission, a one-bounce ray-tracing method is used to track the exact projection of the window (beam illuminance) on the floor, which is then treated as an extra surface with initial luminous exitance in the radiosity calculations. For diffuse daylight, the window interior surface is considered as diffuse luminous source emitting daylight uniformly towards all directions. The calculation model treats the situation by identifying whether the window projection is on floor. If not, the window has an initial luminous exitance equal to the total transmitted illuminance, otherwise the window has an initial luminous exitance equal to the transmitted diffuse illuminance and the floor has the remaining part of transmitted direct illuminance. By making such an assumption, the room is modeled by eight surfaces: the window, the non-lit part of floor, the ceiling, the two sidewalls, the wall containing the window, the back wall, and the window (sunlit) projection on floor. The window and its projection on the floor have variable luminous exitances depending on the solar position and sky conditions. The final luminous exitance of all interior surfaces after inter-reflections in the room are then calculated via radiosity method (Goral *et al*., 1984).

$$M=(I-T)^{-1}\cdot M_0 \tag{1}$$

where M_0 is the initial (source) luminous exitance matrix, I is the 8×8 identity matrix and T is a matrix whose elements are given by $T_{ij}=r\cdot F_{ij}$, F_{ij} being the view factor from surface i to surface j.
The illuminance for representative points on the work plane can be calculated by:

$$E=\Sigma M_i\cdot C_i \tag{2}$$

where C_i is the configuration factor between the investigated point and interior surface i. Note that this entire calculation is done for each hour in the year for a pre-selected grid on the work plane surface.

2.3 Hourly calculation of variable view factors between all interior surfaces

The model calculates the window projection (sunlit area) on the floor. The shape, position and size of window projection vary with time in a day and day number, and hence the view factors between all interior surfaces change every hour. In order to calculate these varying view factors, the geometry shown in Figure 1(a) was used in Cartesian coordinates. The origin is at the lower right corner of the wall containing the window.

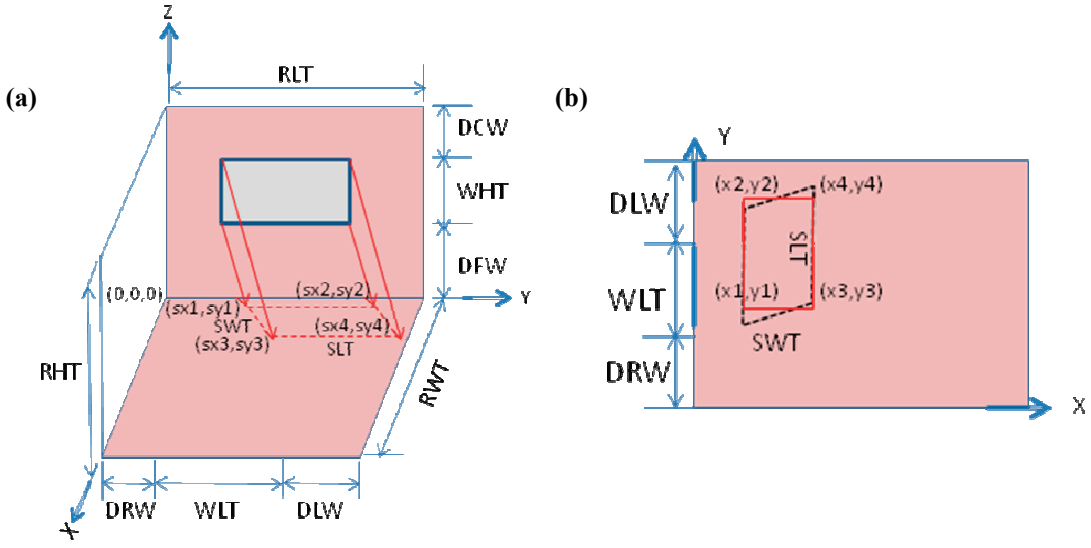

Figure 1: (a) Coordinate system and window projection on floor (b) Equivalent sunlit floor area using a rectangle approximation

Since it is quite complicated and time consuming to calculate the view factors between the window projection and other interior surfaces using the actual shape of the sunlit area, the model transforms the shape of the sunlit area to an "equivalent" rectangle of equal area so that view factors can be computed faster without noticeable errors (Figure 1b). The hourly coordinates of the projected sunlit area on the floor can be calculated using the following equations:

$$\begin{bmatrix} sx1_{n,t} = sx2_{n,t} = \dfrac{DFW}{\tan(\alpha_{n,t})} \cdot \cos(\gamma_{n,t}) \\ sx3_{n,t} = sx4_{n,t} = \dfrac{DFW + WHT}{\tan(\alpha_{n,t})} \cdot \cos(\gamma_{n,t}) \\ sy1_{n,t} = DRW - \dfrac{DFW}{\tan(\alpha_{n,t})} \cdot \sin(\gamma_{n,t}) \\ sy2_{n,t} = DRW + WLT - \dfrac{DFW}{\tan(\alpha_{n,t})} \cdot \sin(\gamma_{n,t}) \\ sy3_{n,t} = DRW - \dfrac{DFW + WHT}{\tan(\alpha_{n,t})} \cdot \sin(\gamma_{n,t}) \\ sy4_{n,t} = DRW + WLT - \dfrac{DFW + WHT}{\tan(\alpha_{n,t})} \cdot \sin(\gamma_{n,t}) \end{bmatrix} \quad (3)$$

where n is day number, t is solar time, α is solar altitude, and γ is the surface solar azimuth. The coordinates of the equivalent projected rectangular are given by:

$$\begin{bmatrix} x1_{n,t} = x2_{n,t} = sx1_{n,t} \\ x3_{n,t} = x4_{n,t} = sx3_{n,t} \\ y1_{n,t} = y3_{n,t} = sy1_{n,t} + \dfrac{sy3_{n,t} - sy1_{n,t}}{2} \\ y2_{n,t} = y4_{n,t} = sy2_{n,t} + \dfrac{sy4_{n,t} - sy2_{n,t}}{2} \end{bmatrix} \quad (4)$$

The hourly dynamic view factors throughout the year can then be obtained after determining the relative coordinates (Eq. (4)) of the sunlit floor area (Murdoch, 2003). For faster computation, the area-weighted reflectance of the exterior (including the window) can be used.

3. MODEL PARAMETERS AND STUDIED VARIABLES

3.1 Building description and representative points on work plane

A typical office space with dimension of 4×4×3m was considered as shown in figure 2. The reflectivities of the window, floor, ceiling and walls are set equal to 0.2, 0.3, 0.8 and 0.5 respectively. The window sill height (DFW: distance from floor to window) is 0.8m, the same as work plane height. The work plane calculation grid consists of 9 points (Figure 2).

3.2 Design variables

Several design variables were considered including building location, window size (expressed as window-to-wall ratio WWR), glass transmittance and orientation. More specifically, this paper includes results for:

(i) Three cities representing different climatic zones in the US are selected: Chicago, New York and Los Angeles;
(ii) Four WWR values: 15%, 30%, 50% and 70% ;
(iii) Three types of glass, with direct visible normal transmittance equal to: 80%, 60% and 40% respectively;
(iv) All four main orientations (south, west, east and north).

The variation of direct glazing transmittance with solar incidence angle is shown in Figure 3.

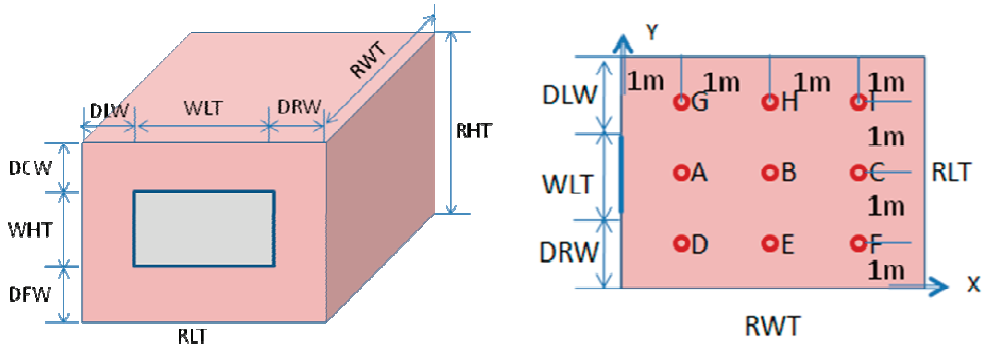

Figure 2. Room geometry and representative points on work plane

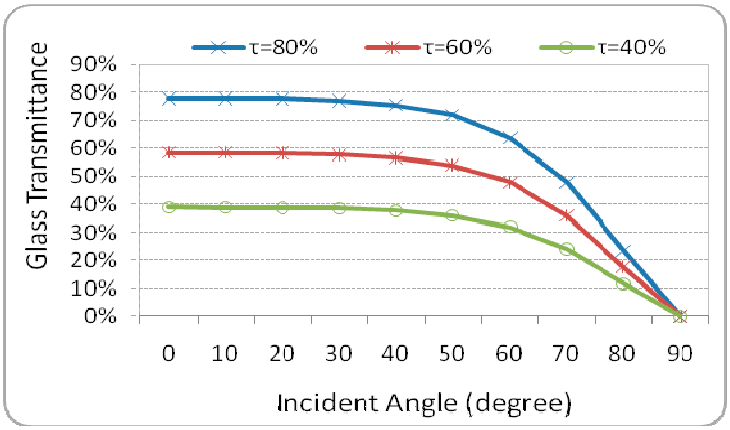

Figure 3. Variation of beam glass transmittance with solar incidence angle

3.3 Daylight performance metrics

Hourly work plane illuminance values are first calculated for the entire year. However, this is a "static" index that cannot be used to describe the overall annual daylighting performance of a specific design since there are 8760 values for each calculation point. Daylight autonomy, an annual measure of how often a minimum work plane illuminance requirement of 500lx (typical set point) can be met by daylight alone, is calculated for the work plane grid for all working hours in the year (9am-5pm). This index includes the impact of all variables (climate, window size and properties, room geometry, etc) and can be also used to predict lighting energy savings if lighting controls are to be used (Tzempelikos and Athienitis, 2007). A limitation of daylight autonomy is that it excludes illuminance values slightly below the threshold (that are useful) and that it does not consider the problem of glare due to excessive daylight. Hence, another metric called useful daylight illuminances is also calculated. It defines the illuminances that fall within the range of 100-2000lx as useful daylight illuminances (Nabil and Mardaljevic, 2005; Nabil and Mardaljevic, 2006). In this study, in order to systematically investigate the work plane illuminance profiles we subdivide the range of useful daylight illuminance into three bins: 100-500lx, 500-1000lx and 1000-2000lx. Finally, two more parameters were computed that could be useful for future glare index estimation and for thermal analysis:

(i) The minimum horizontal distance between the sunlit area (projected on the work plane) and the façade;
(ii) The percentage of directly illuminated floor area.

4. RESULTS AND DISCUSSION

The calculated results are presented in comparative tables and graphs below. The impact of location, WWR, glazing transmittance and orientation were examined in detail. Table 1 shows the average annual daylight autonomy and useful daylight illuminance ratios (on work plane) for a south facing facade. Los Angeles has the highest daylight autonomy and useful daylight illuminance ratio. Chicago ranks second and New York third. This is because Los

Angeles locates at lower latitude and its climate is subject to a large amount of sunshine hours. In each location, daylight autonomy increases with the increase of window to wall ratio and glazing transmittance (also see Figure 4). However, useful daylight illuminance ratio presents more complex and interesting trends. Within UDI bin 1(100-500lx), UDI ratio decreases when window size and glazing transmittance increase. In UDI bin 2(500-1000lx), maximum UDI ratio appears at glazing transmittance equal to 60% for 15% window to wall ratio, and at 80% for other window size options. Also, the UDI ratio decreases with the increase of window size when transmittance is 80% or 60%, but maximizes at 30% window to wall ratio when the glazing transmittance is equal to 40%. In UDI bin 3(1000-2000lx), similar but more complex trends can be observed.

Table 1: Variation of average daylight autonomy and useful daylight illuminances with the studied variables

Location	**New York**			**Chicago**			**Los Angeles**			
WWR	80%	60%	40%	80%	60%	40%	80%	60%	40%	**τ**
15%	72.2	63.1	45	73.8	63.3	47.6	82.6	70.9	52.3	**DA (%)**
30%	89.2	84	73.6	91.7	86.8	76.2	95.3	92.9	85.1	
50%	94.3	91.8	85.5	95.4	93.8	88.6	97.3	96.2	93.7	
70%	96	94.3	90.2	96.4	95.4	92.6	98	97.2	95.6	
15%	24.1	31.4	43.5	23	32.6	48.3	15.8	26.7	43.7	**UDI (%) 100-500lx**
30%	8.9	13.6	22.9	6.6	11	30.4	4.5	6.5	13.4	
50%	4.2	6.6	12.2	3.7	4.9	9.3	2.7	3.8	5.8	
70%	2.7	4.2	7.9	2.9	3.7	5.8	2	2.8	4.3	
15%	24.6	26.8	24.9	28.8	29.4	25	30.3	30.9	27.6	**UDI (%) 500-1000lx**
30%	15.5	19.1	25.2	15.5	22	30.9	10.1	19.1	31.2	
50%	8.8	12.9	18.5	6.8	11.9	20.8	3.6	6	16.4	
70%	5.7	9	14.8	3.8	6.6	14.6	2.4	3.5	8.3	
15%	24.9	21.6	14.9	25	20.6	12.6	27.6	24.4	16.7	**UDI (%) 1000-2000lx**
30%	25.2	29.1	26.9	30.9	32.2	26.5	31.2	33.6	30.7	
50%	18.5	22.9	29	20.8	27.8	33.2	16.4	27.6	35.5	
70%	14.8	19.1	25.2	14.6	21.6	31.3	8.3	16.7	32.2	

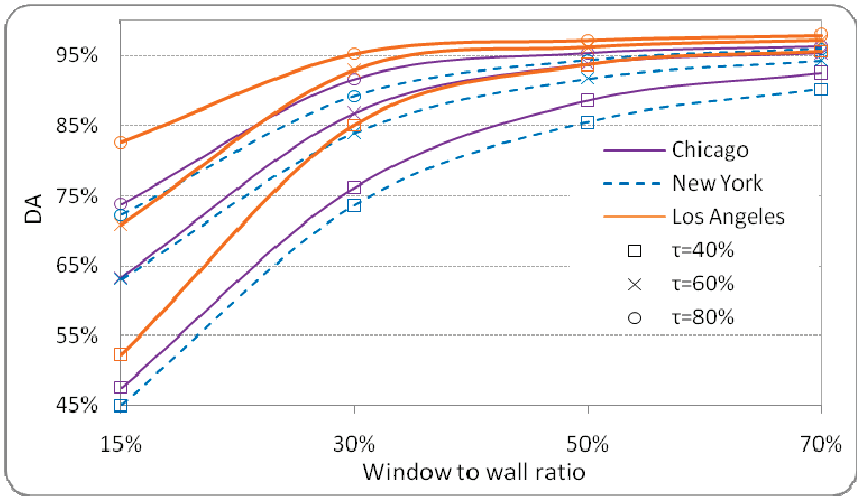

Figure 4. Daylight autonomy as a function of window to wall ratio for three locations and three glazing types

Orientation is another important variable and greatly affects the daylight autonomy as shown in Figure 6. As expected, daylight autonomy is highest when the façade is facing south. For each orientation, the daylight autonomy increases with the increase of window-to-wall ratio and glazing transmittance. However, Fig. 6 shows that for such a typical private office, 40% window-to-wall ratio is enough to exploit daylight since there is no significant increase in daylight autonomy for larger window size. This result is consistent with those of similar studies for other climates (Tzempelikos and Athienitis, 2007).

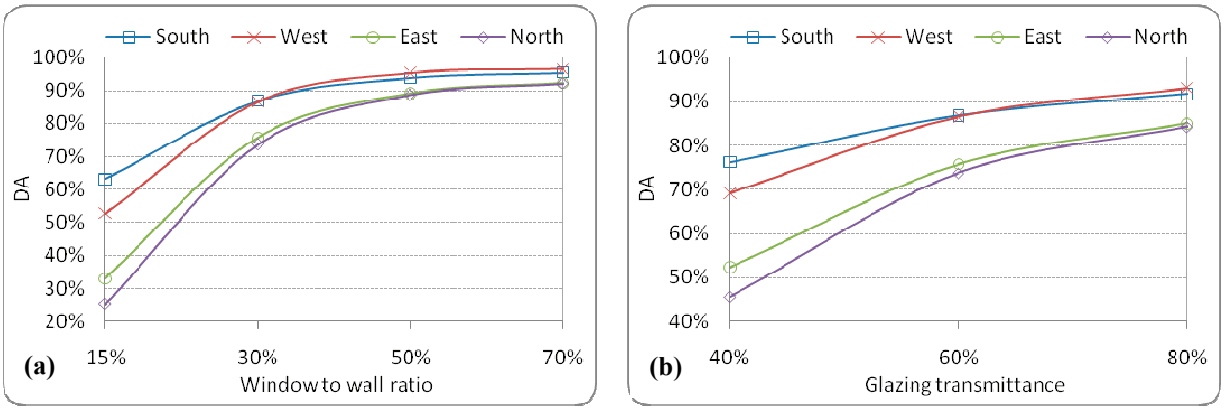

Figure 6. Daylight autonomy as a function of (a) window-to-wall ratio (left, τ=60%) and (b) of glazing transmittance (right, WWR=30%) for four main orientations in Chicago.

The authors believe that the amount of daylight falling in the range between 500lx and 1000lx is the most useful since it can offset electric lighting without causing glare; therefore, the useful daylight illuminance ratio is plotted as a function of window-to-wall ratio and glazing transmittance within UDI bin 2 for each orientation, (Figure 7).

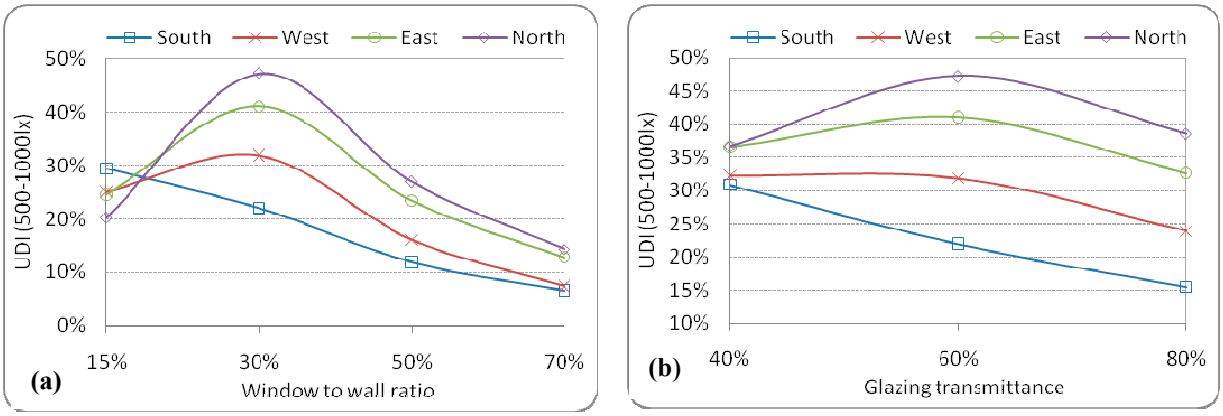

Figure 7. (a) Useful daylight illuminance ratio as a function of window-to-wall ratio (left, τ=60%) and (b) as a function of glazing transmittance (right, WWR=30%) for four main orientations in Chicago.

With the increase of window size, UDI ratios show similar trends for all orientations except south –they first increase to maximum values at 30% window size and then decrease gradually to around 10-15%. As for south facing windows, the UDI ratio continually decreases with the increase of window size. This is explained by the fact that south windows receive much more daylight than other orientations, so when window size increases, the average illuminance on work plane may increase to more than 1000lx and thus decreases the UDI ratio for this bin. As to the other three orientations, a larger window size also increases the average illuminance and excludes some hours just below the upper limit of 1000lx out of the daylight illuminance range. But the window size increase brings more hours when otherwise may below the lower limit of 500lx into the daylight illuminance range. This explains why UDI ratios reach a maximum values around 30% WWR. Similar trends can be seen when the glazing transmittance changes (Figure 7b).

Glare is always a problem in perimeter spaces with windows (Kim *et al*., 2007). In the absence of shading devices (which are essential) proper arrangement of work space positions is important to reduce visual discomfort. Areas that are frequently sunlit should be avoided. Figure 8 shows the maximum and minimum horizontal distance between the sunlit area on floor and the facade during three representative days. For a given room, larger solar altitude or larger surface solar azimuth would result in smaller distances. Whether the distances become larger or smaller depends on the combination effects of solar altitude and surface solar azimuth. In general, the sunlight enters into the deep part of a space due to lower solar altitude in winter. And in summer, the solar altitude is high, so the

sunlight only enters into a small part of the space. In the morning and afternoon, lower solar altitude may result in larger distance. But at that time, the surface solar azimuth is also large which has adverse effect on the distance. From one hour to the next, whether the distances become larger depends on which of the two angles plays the key role. As show in Figure 8, in winter solar altitude plays more important role, so the minimum distance has two peaks at near 9AM and 15PM with a smaller value in noon. In summer, surface solar azimuth overwhelms solar altitude, so the maximum distance appears near noon.

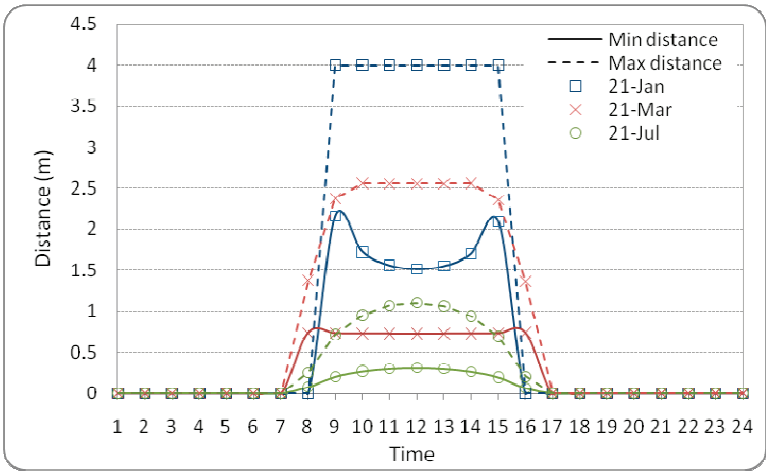

Figure 8: Maximum and minimum horizontal distance between sunlit area and a south-facing façade in Chicago.

The last calculated parameter, the fraction of sunlit area of the work plane surface is shown for every hour in the year in Figure 9. Higher values are realized in winter because of low solar altitude angles. They maximize around noon, since for early morning and late afternoon the window projection is on the side walls instead of the work plane surface (or floor).

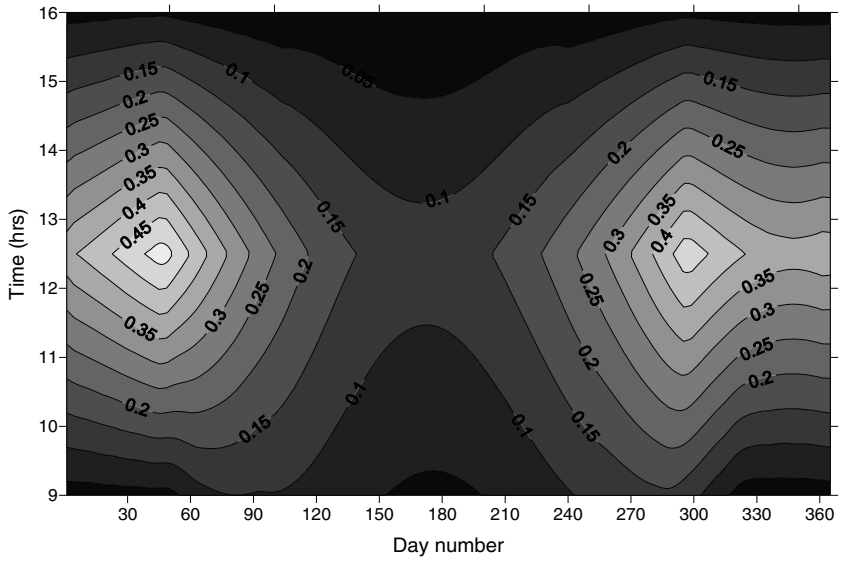

Figure 9: Fraction of directly illuminated work plane area throughout the year for a south-facing façade in Chicago.

5. CONCLUSIONS

This paper presents a daylighting calculation model using hourly data and a combined radiosity/ray-tracing method. Direct and diffuse daylight are treated separately: when direct daylight is present, the projected sunlit area on the

floor is calculated and treated an as an extra surface with initial luminous exitance for later radiosity calculations. For diffuse light, the window is assumed a Lambertian source. Daylight autonomy and useful daylight illuminance are measures that provide important information for the daylighting conditions throughout the year. Using dynamic (variable) view factors, these metrics were computed as a function of façade parameters (window size, properties, orientation and geometry) in order to help the designers make better decisions related to optimal daylighting performance. Results were presented for 3 different locations in the US. The distance between the facade and sunlit area on floor and the fraction of sunlit area were also computed n an hourly basis. This study is the starting point for a future model that will include the impact of shading for a complete evaluation of overall daylighting performance of office spaces.

REFERENCES

American Society of Heating, Refrigeration and Air-Conditioning, 2007, *ASHRAE Handbook-Fundamentals,* Atlanta, USA.

Carrol, WL. 1999, Daylighting simulation: methods, algorithms, and resources, a report of IEA SHC Task21/ECBCS ANNEX 29 and Lawrence Berkeley National Laboratory LBNL-44296.

Goral, C., Torrance, K., Greenberg, D., Battaile, B., 1984, Modeling the interaction of light between diffuse surfaces. *Computer Graphics*, vol. 18, no. 13: p.213-222.

Kim, K., Kim, B.S., Park, S., 2007, Analysis of design approaches to improve the comfort level of a small glazed-envelope building during summer, *Solar energy*, vol. 81, no. 1: p. 39-51.

Mardajevic, J., 2001, The BRE-IDMP dataset: a new benchmark for the validation of illuminance prediction techniques, Lighting *Research and Technology*, vol. 33, no 2: p. 117-136.

Murdoch, J., 2003, *Illuminating engineering: from Edison's lamp to the LED*, 2nd edition, Visions Communications, New York, USA, 750 p.

Nabil, A., Mardaljevic, J., 2005, Useful daylight illuminances: a new paradigm for assessing daylight in buildings, *Lighting Research and Technology,* vol. 37, no 1: p. 41-57.

Nabil, A., Mardaljevic, J., 2006, Useful daylight illuminances: a replacement for daylight factors, *Energy and* Buildings, vol. 38: p. 905-913.

National solar radiation data base typical meteorological year 3 database: http://rredc.nrel.gov/solar/old_data/nsrdb/1991-2005/tmy3/by_state_and_city.html

Perez, R., Ineichen, P., Seals, R., 1990, Modeling daylight availability and irradiance components from direct and global irradiance. *Solar Energy*, vol. 44, no. 5: pp. 271-289.

Reinhart, C., 2002, The annual daylight availability in peripheral offices in Canada –a simulation study, National Research Council of Canada, *Report #44-B3213-L*.

Reinhart, C., Mardaljevic, J., Rogers, Z., 2006, Dynamic Daylight Performance Metrics for Sustainable Building Design, *LEUKOS,* vol. 3, no.1: p. 1-25.

Rosa, A., Ferraro, V., Igawa, N., Kaliakatsos, D., Marinelli, V., 2009, INLUX: A calculation code for daylight illuminance predictions inside buildings and its experimental validation. *Building and Environment*, vol. 44: p. 1769-1775.

Lawrence Berkeley National Laboratory, 1994, Predicting daylighting and lighting performance in complex building spaces: *SUPERLITE 2.0*, University of California, USA.

Tzempelikos, A., Athienitis, A.K., 2002, Investigation of lighting, daylighting and shading design options for new Concordia University engineering building. In: *Proceedings of eSim2002 Building Simulation Conference,* Montreal, Canada, p. 177-184.

Tzempelikos, A., Athienitis, A.K., 2007, The impact of shading design and control on building cooling and lighting demand, *Solar Energy*, vol. 81: p. 369-382.

Ward, G., Shakespeare, R., 2003, *Rendering with RADIANCE: the art and science of lighting visualization*, Space and Light, California, USA.